A Path toward SARS-CoV-2 Attenuation: Metabolic Pressure on CTP Synthesis Rules the Virus Evolution

Zhihua Ou[1,2], Christos Ouzounis[3], Daxi Wang[1,2], Wanying Sun[1,2,4], Junhua Li[1,2], Weijun Chen[2,5,*], Philippe Marlière[6], and Antoine Danchin [ID][7,8,*]

[1]BGI-Shenzhen, Shenzhen, China

[2]Shenzhen Key Laboratory of Unknown Pathogen Identification, BGI-Shenzhen, Shenzhen, China

[3]Biological Computation and Process Laboratory, Centre for Research and Technology Hellas, Chemical Process and Energy Resources Institute, Thessalonica, Greece

[4]BGI Education Center, University of Chinese Academy of Sciences, Shenzhen, China

[5]BGI PathoGenesis Pharmaceutical Technology, BGI-Shenzhen, Shenzhen, China

[6]TESSSI, The European Syndicate of Synthetic Scientists and Industrialists, Paris, France

[7]Kodikos Labs, Institut Cochin, Paris, France

[8]School of Biomedical Sciences, Li KaShing Faculty of Medicine, Hong Kong University, Pokfulam, Hong Kong

*Corresponding authors: E-mails: antoine.danchin@normalesup.org; chenwj@bgi.com.

Abstract

In the context of the COVID-19 pandemic, we describe here the singular metabolic background that constrains enveloped RNA viruses to evolve toward likely attenuation in the long term, possibly after a step of increased pathogenicity. Cytidine triphosphate (CTP) is at the crossroad of the processes allowing SARS-CoV-2 to multiply, because CTP is in demand for four essential metabolic steps. It is a building block of the virus genome, it is required for synthesis of the cytosine-based liponucleotide precursors of the viral envelope, it is a critical building block of the host transfer RNAs synthesis and it is required for synthesis of dolichol-phosphate, a precursor of viral protein glycosylation. The CCA 3′-end of all the transfer RNAs required to translate the RNA genome and further transcripts into the proteins used to build active virus copies is not coded in the human genome. It must be synthesized de novo from CTP and ATP. Furthermore, intermediary metabolism is built on compulsory steps of synthesis and salvage of cytosine-based metabolites via uridine triphosphate that keep limiting CTP availability. As a consequence, accidental replication errors tend to replace cytosine by uracil in the genome, unless recombination events allow the sequence to return to its ancestral sequences. We document some of the consequences of this situation in the function of viral proteins. This unique metabolic setup allowed us to highlight and provide a *raison d'être* to viperin, an enzyme of innate antiviral immunity, which synthesizes 3′-deoxy-3′,4′-didehydro-CTP as an extremely efficient antiviral nucleotide.

Key words: ABCE1, cytoophidia, Maxwell's demon, Nsp1, phosphoribosyltransferase, queuine.

Significance

As COVID-19 expands its course, the genome of SARS-CoV-2 evolves. It is deficient in one of the four genomic bases, cytosine. Here, we establish that when it multiplies, the virus taps into metabolic resources shaped by the availability of cytosine triphosphate (CTP), setup to be limiting to coordinate the cell's metabolism. This nucleotide is uniquely required not only for genome synthesis but also for synthesis of the virus envelope, translation (via addition of a CCA end to transfer RNA), and glycosylation of its proteins (via a terpene anchor binding to the endoplasmic reticulum). Innate antiviral immunity has evolved to generate a toxic analog of CTP, paving the way for the design of novel synthetic inhibitors of the virus development.

Introduction

The COVID-19 pandemic motivated a deluge of literature investigating how the SARS-CoV-2 coronavirus develops and evolves. Molecular analyses of the virus' genome and of its proteins keep accumulating at a fast pace (https://viralzone.expasy.org/8996 last accessed November 9, 2020). Surprisingly, the way the virus taps into its cell host's metabolism to build up its genome, proteins, and envelope is seldom explored. We investigated here how unique metabolic features impact on the virus' functions, aiming at understanding and possibly revealing conditions for alleviation of its virulence. Coronavirus genomes mimic the structure of cellular mRNAs, beginning with a conventional 5'-end methylated cap (Jin et al. 2013) and ending up with a 3'-polyadenylated tail. Although remarkably apt to create a stealthy mRNA mimic, the SARS-CoV-2 genome is so similar to that of the host's mRNAs that standard interference with the virus expression machinery will often also interfere with that of noninfected cells and be toxic to the host. The virus is also an enveloped virus. Both of these attributes imply drawing resources from the cell's nucleotide and lipid metabolism.

A noteworthy feature shared by the viral envelope construction and genome synthesis is that both rely on CTP availability. This prompted us to analyze the consequences of the nucleotide requirement for these processes, as compared with the host cell's metabolism that ends up as cellular mRNAs and membranes. We previously pointed out how a series of events which begins with copying the virus positive-sense RNA into a general template minus-sense RNA that serves to generate new viral genomes and several individual transcripts of that template (Sawicki et al. 2007; Chen et al. 2020) is tightly linked to the metabolism of cytosine-containing nucleotides (Danchin and Marlière 2020). We further develop here the singular role of CTP, in particular in its mandatory requirement for transfer RNA (tRNA) maturation into a functional entity, as this impacts availability of a functional translation machinery, exploring the phylogenetic consequences of this metabolic setup. It had been noticed that the virus exploits a critical set of pyrimidine-related metabolic pathways to access the pool of ribonucleoside triphosphates needed for the RNA-dependent replication and transcription of the replicated RNA minus strand (Lucas-Hourani et al. 2013). However, the specific role of CTP was overlooked. In fact, CTP is used in four independent processes, all of them essential for the construction of active enveloped RNA viruses. CTP is required not only for 1) construction of the viral genome but also for 2) the construction of a subset of lipid metabolism (Danchin and Marlière 2020), and, as developed here for the first time, 3) for synthesis of active tRNA molecules,

and 4) for protein glycosylation via formation of dolichol-phosphate. This makes the viral sequence highly sensitive to metabolic details of the cell's CTP pool synthesis and maintenance, likely to be reflected in the virus evolution as it mutates with a slow general decrease in cytosine nucleotides, attributed at this time to causes that widely differ from what we present here (Di Giorgio et al. 2020; Xia 2020).

By contrast, functional analysis helped us to reveal unexpected key functions of the virus, marked by a divergent trend in the local content of cytosine nucleotides. For example, if the presence of a subset of amino acids—e.g., proline residues—in viral proteins was essential for key functions required for long-term survival, then a local increase in cytosine residues would expand the evolutionary landscape of the virus. This type of local bias has indeed been highlighted in a previously discovered feature of coronavirus adaptation to the human host: in SARS-CoV-1 a GC-rich critical sequence of the virus spike protein—a leucine to alanine mutation derived from a GC local enrichment, with a UUA codon changed into GCA—displayed positive selection in the course of evolution of the SARS disease in 2003 (Song et al. 2005). Here, we depict first, with emphasis on SARS-CoV-2, the details of cytosine-based metabolism that must be retained as a unique coordinator of the global cell metabolism. We then explore the likely consequences of this dependency on the evolution both of cytosine-related innate immunity processes and of the viral genome sequence. Subsequently, we delineate critical details of the impact on the virus biological functions on the nucleotide composition of its genes and consequences for its short- and long-term evolution.

Results

In-Depth Analysis of Pyrimidine Metabolism Highlights the Unique Position of CTP in Metabolism

To understand how viruses recruit the functions of their host cells to their benefit, we must understand what would be the point of view of a virus if it were to sustain propagation over many generations. Essentially lacking biosynthetic potential, a virus must tap into the host's metabolic resources. This introduces a considerable limitation in the metabolic options offered to viral multiplication. For this reason, many viruses ended up coding for functions that are missing or deficient in their hosts (Moreno-Altamirano et al. 2019). Some even help their hosts to upgrade their built-in ability to make the most of their environment, thus ensuring a wealthy propagation of the viral progeny. Auxiliary metabolic genes are commonplace in bacteriophages (Thompson et al. 2011), but also in a variety of eukaryotic viruses, such as herpes viruses (Hew et al. 2015). Selection pressure via efficacy of transmission multiplied by number of replicates per cell, coupled to
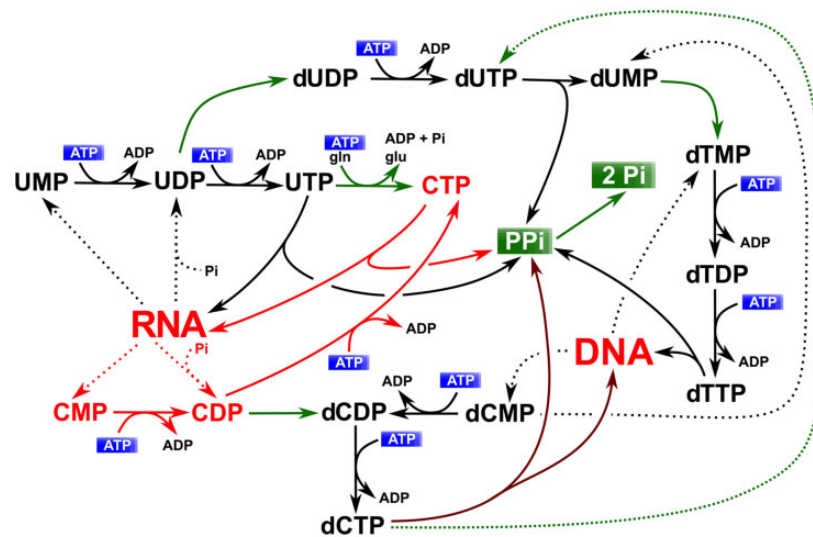
FIG. 1.—Energy-driven pyrimidine-based nucleic acid metabolism. ATP is the general donor in the biosynthesis of pyrimidines. CDP, required as a precursor of dCTP synthesis is produced by RNA turnover via hydrolysis or phosphorolysis (red arrows). RNA and DNA synthesis is driven by pyrophosphate hydrolysis (green arrows indicate irreversible reactions). dTTP results from a pyrophosphate-driven reaction producing dUMP, and is finely tuned by thymidylate kinase, which makes its immediate precursor dTDP.

selection stemming from intracellular availability of essential precursors (nucleotides, amino acids, lipids, and carbohydrates) creates a variety of bottlenecks that shape the virus evolutionary landscape (Kutnjak et al. 2017; Arribas et al. 2018; Orton et al. 2020). Furthermore, the envelope of many animal viruses is built up from components of the host cell's membranes (Pratelli and Colao 2015; Perrier et al. 2019), as well as a capsid made of virus-specific proteins (Li 2016; Schoeman and Fielding 2019). To harden them against environmental offenses and provide them with addressing tags, some of these proteins are glycosylated, which involves tapping into the cell's resources of UDP-sugars and GDP-sugar precursors (Wellen and Thompson 2012; Mayer et al. 2019). The very process of glycosylation via the endoplasmic reticulum requires dolichyl-phosphate, a terpene lipid unexpectedly phosphorylated by CTP-dependent dolichol kinase (Shridas and Waechter 2006). This further highlights the relevance of the membrane lipids, which uniquely derive from precursors involving pyrimidines, specifically liponucleotides based on a CDP skeleton (Kuo et al. 2016; Woods et al. 2016; Lee and Ridgway 2020). As a final key resource, we emphasize here the need for a virus to build up an active tRNA complement in order to express its proteins, necessitating the function of host tRNA-nucleotidyltransferase (CCAse). How the construction of the building blocks is put together in an uninfected cell is therefore the very first challenge faced by the virus after it has accessed the cytoplasm of the host cell. Finding an answer to this question dictates the exploration of the mystery of the cells' assembly lines that prepare them for growth. Before exploring phylogenetic consequences of

this unique design, we propose in the next couple of paragraphs an integrated view of how cytosine-based metabolism is organized.

The Logic of Energy Management for Nucleic Acids Synthesis

Synthesis of the viral RNA genome draws resources not only from the metabolism of pyrimidines but also from the general logic of the cell's energy management. A key chemical feature of the related processes is that they rest on hydrolysis or synthesis of phosphate bonds (Westheimer 1987). Versatility of these processes is ensured by the usage of the shortest polyphosphate structure, that of nucleoside triphosphates, NTPs—we do not consider here the special case of purely mineral polyphosphates (Danchin 2009). RNA- and DNA-dependent genome synthesis is developed along two lines with respect to its energy demands (this is illustrated in fig. 1 for pyrimidine metabolism).

When energy is meant to be used in a reversible way, NTPs are hydrolyzed into NDP + Pi. This is where the role of mitochondria is critical, especially in nonproliferating cells (Maldonado and Lemasters 2014). These organelles restore the ATP complement of the cell, in particular to the endoplasmic reticulum—ER, (Yong et al. 2019), and in the present context this is crucial for the generation of new viral particles. In contrast—and this is relevant not only for intermediary metabolism but also for macromolecule biosynthesis, with >500 such reactions reported in the KEGG database (Kanehisa et al. 2017)—when the relevant pathways have to be driven

forward, triphosphate hydrolysis produces pyrophosphate (PPi). PPi is subsequently hydrolyzed irreversibly into two phosphates by omnipresent pyrophosphatases: $NTP => NMP + PPi => NMP + 2 Pi$, and this drives syntheses forward. Biosynthesis of macromolecules rests to a great extent on this two-pronged strategy. In parallel, the requirement of CDP for synthesis of the deoxyribonucleotide counterpart (fig. 1) limits the input of C nucleotides in DNA-based genomes (Rocha and Danchin 2002). Are RNA viruses also submitted to patent metabolic constraints, and what would they be?

An Unexpected Secret of Life: Cytosine Metabolism Provides Both a Rheostat and a Flywheel to Integrate Growth of the Various Cell Structures, Constraining Coronavirus Development

Surprisingly, the answer to this question is positive, with the involvement of cytosine nucleotides, again. All metabolites must be degraded and recycled, either as a whole or as parts. In the case of ribonucleotides, three units—a phosphate, a ribose, and a heterocyclic base—can go through specific degradation or salvage pathways. Strikingly, cytosine appears to sustain a privileged turnover metabolism, entirely poised to go via deamination to uracil, so that most of the cytosine nucleotide metabolism should go through phosphorylated forms, CMP and CDP for salvage, and CTP for de novo biosynthesis. Further in line with a general cytosine-based control, a specific pathway forms cytidine after hydrolysis of the 5′-phosphate of CMP, then deaminates it to uridine (Frances and Cordelier 2020), or, in bacteria but not in multicellular organisms, makes cytosine, which is subsequently deaminated to uracil (Ireton et al. 2002), then mainly scavenged directly by uracil phosphoribosyltransferase (UPRT, EC 2.4.2.9, fig. 2 blue arrow) directly into UMP. That this indirect route plays a crucial role in cells is witnessed, for example, in the fact that the whole RNA-derived salvage pathway (cytidylate phosphatase and cytidine deaminase) is critical in embryonic development (Wegelin 1983). Furthermore, the very same enzymes of this salvage pathway are also important to recycle the modified derivatives of cytosine which result from frequent metabolic accidents or are encountered as epigenetic markers (Zauri et al. 2015).

Thus, the salvage pathways are straightforward for all nucleobases, cytosine excepted (table 1).

The purine salvage pathways have been thoroughly explored, in particular in animal pathogens and in plants (Ghérardi and Sarciron 2007; Ducati et al. 2011; Ashihara et al. 2018). By contrast, the pyrimidine salvage pathways have remained somewhat less studied (Villela et al. 2011). The omnipresent roles of ATP and S-adenosylmethionine (AdoMet) often end up with adenine as a waste product. As a consequence, natural selection retained a variety of enzymes meant to scavenge adenine wastes, so that any

downward trend in the ever-critical ATP supply would be easily overcome (Lüscher et al. 2014; Sekowska et al. 2019). A key enzyme in this salvage process is adenine phosphoribosyltransferase (EC 2.4.2.7; Wilson et al. 1986; 1,290 references in PubMed on September 25, 2020). In the same way, guanine (respectively, uracil) are salvaged via (hypoxanthine)-guanine phosphoribosyltransferase (EC 2.4.2.8; Balendiran et al. 1999; 1,545 references in PubMed on September 25, 2020), (respectively UPRT, EC 2.4.2.9; Li et al. 2007; 312 references in PubMed on September 25, 2020). Further comparable activities exist, such as orotate phosphoribosyltransferase EC 2.4.2.10 (Donini et al. 2017)—which inputs orotate at the beginning of the pyrimidine biosynthetic pathway—and the somewhat less similar nicotinamide phosphoribosyltransferase EC 2.4.2.12 (Grolla et al. 2020). These enzymes share a common descent, showing that life has easily evolved a panoply of related activities.

It was therefore expected that the same would hold true for cytosine, allowing the cell to scavenge the base easily from its environment. Yet, we made the unexpected discovery that, to the best of our knowledge, no cytosine phosphoribosyltransferase exists in any extant organism (light blue arrow, fig. 2). This apparent deficiency might result from some moonlighting activity of UPRT allowing it to recognize cytosine. However, this is unlikely. For example, in the minimal genome of *Mycoplasma mycoides* UPRT and cytidine 5′-triphosphate synthetase determine the rate of pyrimidine nucleotide synthesis, implying that there is no direct scavenging cytosine into CMP (Mitchell and Finch 1979). UPRT in *Escherichia coli* is highly specific for uracil and some uracil analogs (Rasmussen et al. 1986). The same is true in plants with a moonlighting enzyme that does not lead to CMP (Katahira and Ashihara 2002; Arrivault 2019), whereas mammals were supposed to lack this activity altogether (Cleary et al. 2005), until a structurally related protein was identified, although failing to display UPRT activity (Ghosh et al. 2015). Finally, the fact that pyrimidine metabolism flows essentially through uracil, not cytosine derivatives has been established in parasites (Dai et al. 1995; Schumacher 1998). By contrast, early work with the protozoon *Giardia lamblia* suggested that this activity might be present in the organism (Aldritt et al. 1985; Jarroll et al. 1989). Surprisingly, however, deciphering the genome strongly suggested that CTP was derived from cytosine deamination into uracil, followed by salvage of uracil and amidation. Indeed in the most recent release of GiardiaDB, there appears to be no sequence in the genome of the organism that could be attributed to cytosine phosphoribosyltransferase (see Aurrecoechea et al. [2009] for access to the genome database). At this point, therefore, no known extant organism codes for such an enzyme. By contrast, despite the lack of de novo biosynthesis pathways for pyrimidines in this organism, the genome still codes for a CTP synthetase (PyrG). This is in line with the general observation that cytosine and related cytosine-containing derivatives are
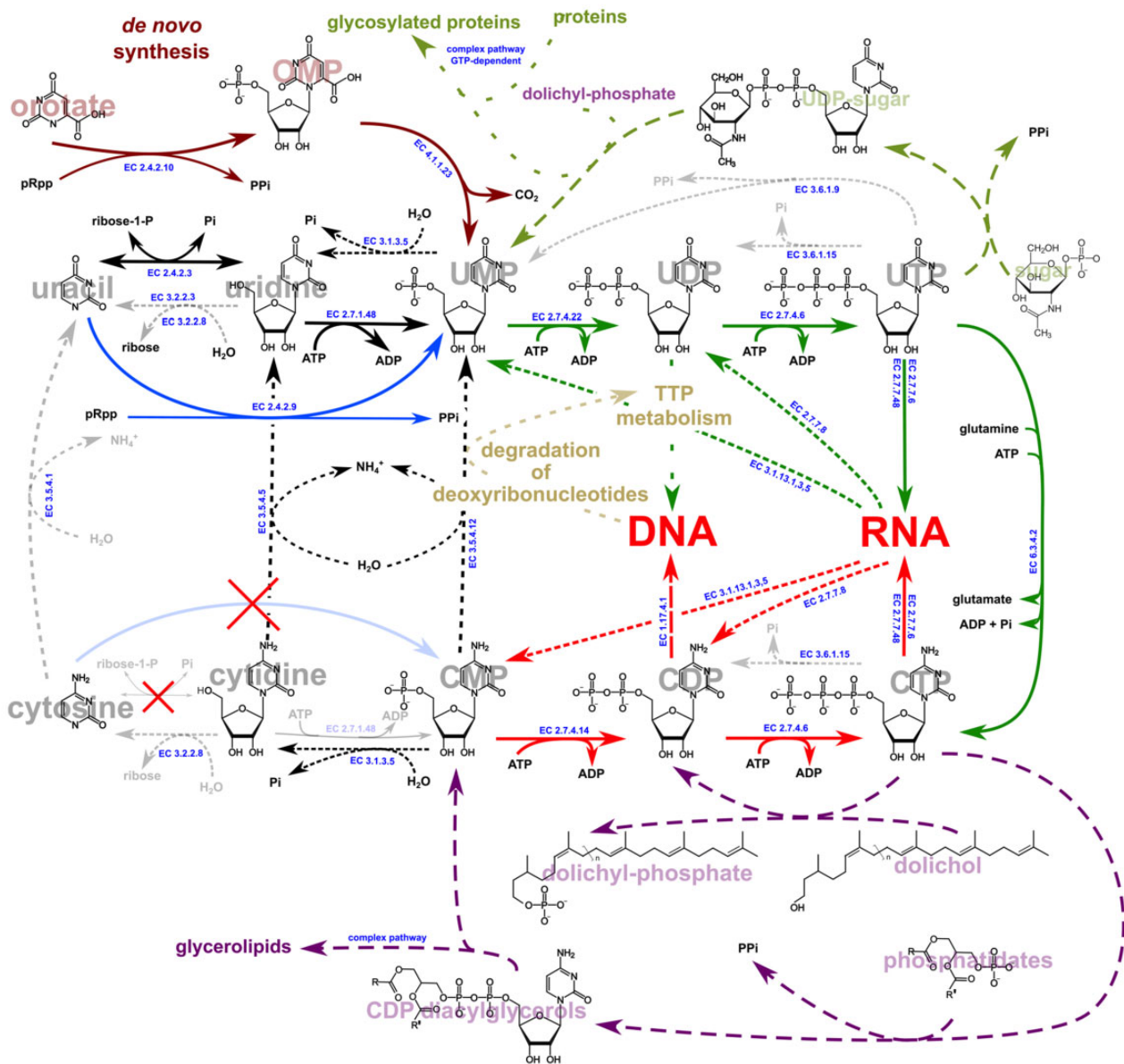
FIG. 2.—Synthesis and salvage of pyrimidine nucleotides. Synthesis of UMP begins with orotate phosphoribosyltransferase followed by decarboxylation (brown arrows). The anabolic pathway ends up with uridine triphosphate and CTP (bright green arrows). Salvage of CTP stems from RNA metabolism (red arrows) and lipid metabolism (purple arrows). Degradation and scavenging of cytosine-based nucleotides go through uracil-based scavenging and return to the CTP biosynthetic pathway, with cytosine deamination of intermediates as critical steps. UPRT matches the role of the orotate counterpart in the ultimate salvage of the base (blue arrow). No counterpart has been yet identified, to our knowledge (see text), for scavenging cytosine (crossed out light blue arrow). Distribution of relevant enzymes in *Homo sapiens* and model bacteria is illustrated in table 1.

systematically deaminated into uracil-containing derivatives, subsequently processed to regenerate CTP (fig. 2, and fig. 1 for salvage of processed DNA derivatives). As a further case in point, *pyrG* has also been found as a necessary complement required for life in the smallest genome of an autonomous synthetic streamlined construct (Hutchison et al. 2016). This strongly suggests that recovering CTP requires a uracil-dependent pathway as well as that independent

management of cytosine-based nucleotides is critical to govern metabolism, even in the presence of a rich supply of metabolites from the outside—note that *Giardia* is a parasite.

This singular positioning of CTP synthesis in metabolism makes CTP synthetase a convenient enzyme for the cell to adjust the flow of cytosine-containing nucleotides, acting as a rheostat does in an electric contraption (Shin et al. 2020). Substantiating this unique role, the functional structure of

Table 1

Cytosine-Related Salvage in Human Cells: Present and Missing Enzymes with Bacteria for Comparison

	Homo sapiens	*Escherichia coli*	*Bacillus subtilis*	Enzyme Name
Catabolism				
3.5.4.12	DCTD	absent	*comEB*	dCMP/CMP deaminase
3.1.3.5	NT5E	*umpG*	*nucF(yutF)*	5′-nucleotidase
	NT5C3	*pynN(yjjG)*	*pynN(yfnB) ycsE*	
	NT5C1A		*yktC*	
3.5.4.5	CDA	*cdd*	*cdd*	Cytidine deaminase
3.5.4.1	Absent	*codA (cda)*	Absent	Cytosine deaminase
3.2.2.8	Absent	*rihA(ybeK) rihB(yeiK) rihC(yaaF)*	Absent	Ribosylpyrimidine nucleosidase
Synthesis				
6.3.4.2	CTPS1	*pyrG*	*pyrG*	CTP synthetase
	CTPS2			
Salvage				
2.7.4.14	CMPK1	Absent	Absent	UMP/CMP kinase
	CMPK2			
2.7.4.25	Absent	*cmk*	*cmk*	Cytidylate kinase
Recovery from U				
2.4.2.3	UPP1	*udp*	*pdp*	Uridine phosphorylase
	UPP2			
2.4.2.9	UPRT	*upp*	*upp*	Uracil phosphoribosyltransferase
2.7.1.48	UCK1	*udk*	*udk*	Uridine kinase
	UCK2			
	URKL1			
2.7.4.22	Absent	*pyrH*	*pyrH*	Uridylate kinase
2.7.4.6	NME1–NME7 (7 genes)	*ndk*	*ndk*	Nucleoside diphosphate kinase

the enzyme displays a very unusual architecture. It makes filaments, named cytoophidia—specific membrane-less organelles that control the spatial distribution of cytosine-dependent intermediary metabolism (Liu 2010; Sun and Liu 2019)—in all the organisms where its organization has been explored (Li et al. 2018). The structure of CTP synthetase is important in the present context because the synthesis of membrane lipids is a further metabolic step that involves the nucleotide, with most membranes deriving from cytosine-based liponucleotides (Chauhan et al. 2016; McMaster 2018). Because the lipid content of cells can vary over a wide range, the stores of CDP-containing liponucleotides, in particular in eukaryotes—with an important network of intracellular membranes—is preset to play the role of a flywheel, allowing fine tuning of the availability of cytosine-derived metabolites in the cell when conditions vary. This property could have been advantageously recruited for innate immunity. Indeed, inactivation of one of the two human CTP synthetase genes strongly impaired lymphocyte function (Martin et al. 2020). Finally, as perhaps could be expected at this point of our demonstration, the very first enzymes for de novo synthesis of pyrimidines, carbamoyl-phosphate synthetase (CPSase), aspartate transcarbamylase (ATCase), and dihydroorotase (DHOase) are associated into a multifunctional structure, named CAD (Del Caño-Ochoa and Ramón-Maiques 2020). Besides a general role in management of cell growth, CAD is highly expressed in leukocytes, where it enables Toll-like receptor 8 expression in response to cytidine

and single-stranded RNA (Furusho et al. 2019), a situation met upon infection by RNA viruses. Supporting a role of CAD in antiviral innate immunity, its activity is modulated by a dedicated viral protein during Enteroviral infection (Cheng et al. 2020).

As a matter of fact, most enveloped RNA viruses are low in C. When viruses of the same genus are vector-borne, they appear to display a different nucleotide composition, sometimes higher in $G + C$ (Jenkins et al. 2001), indicative of some driving force due to the metabolism of the vector, not investigated at this time. There are also some specific examples of $G + C$-rich viral genomes such as that of the Rubella virus (Zhu et al. 2016). The reason for this exceptional nucleotide composition is not known, and it has been attributed to inhibition of the APOBEC1-editing process (Khrustalev and Barkovsky 2011). However, such inhibition would require a specific viral function, a feature that we rather propose to see involved in modulating either CAD activity (as discussed above for enteroviruses) or preferably CTP synthetase. Our observations would therefore be extremely helpful in focusing research on identification of viral proteins interfering with cytoophidia.

Consequences of Cytosine-Related Imbalance in Nucleotide Composition, Evolution, and Coding Capacity of Coronavirus Genomes

The most straightforward consequence of the metabolic qualitative design just outlined is that a metabolic force will keep driving the cytosine content of RNAs to lower values, unless

opposite processes—and selection pressure leading to discard organisms with too low cytosine content, for example, because this would create unbearable biases in the amino acid composition of the proteins coded by these genomes—had the upper hand during evolution. This prompted us to develop an explicit analysis of the consequences of pyrimidine metabolism's organization in relation with SARS-CoV-2 infection, as we now document.

Cytosine Content-Related Phylogeny of Some Virus Isolates

The constraint on cytosine availability witnessed in the composition of coronaviruses—in particular SARS-CoV-2—is likely to reflect the coupling between synthesis of viral particles and the host cell's metabolic capacity. In order to assess the evolution of the virus with these metabolic constraints we evaluated the C content of their genome, using 89 representative strains from the four genera of coronaviruses, selected based on their phylogenetic and host background. Here, we developed two distinct approaches in order to take into account 1) the nucleotide patterns across the virus group, and 2) the coding sequence-related limitations that constrain the function of the viral proteins as they adapt to their host.

To study the evolution of coronaviruses, we used standard techniques to generate a phylogenetic tree of representative strains (see Materials and Methods), where we highlighted the average cytosine content of each viral genome (supplementary fig. S1, Supplementary Material online). There is significant variation between the cytosine content of viruses of different clades. Based on 89 representative genomes, we found that coronaviruses have 27.3% A, 17.9% C, 21.5% G, and 33.3% U on an average. Overall, the coronavirus genomes contain somewhat more pyrimidines than purines, with a mean content for C + U of ~51.2%.

Currently, seven coronaviruses are known to infect humans. These include four epidemic CoVs causing mild respiratory symptoms in humans (HCoV-229E, HCoV-NL63, HCoV-HKU1, and HCoV-OC43), the severe acute respiratory syndrome coronavirus (SARS-CoV-1) causing the pneumonia outbreak during 2002–2003 in China (Drosten et al. 2003), the Middle East respiratory syndrome coronavirus (MERS-CoV) still causing small outbreaks through camel-to-human transmissions in the Middle East and the newly emerged SARS-CoV-2 (Cui et al. 2019). These viruses all originated from bat species, although the exact intermediate hosts involved in human infections remains obscure (Huynh et al. 2012; Corman et al. 2015; Lau et al. 2015; Yang et al. 2016; Moreno et al. 2017). Interestingly, the cytosine content of bat viruses is variable (from 16.0% to 21.5%), reflecting the diverse virus species harbored by bats, which make a very diverse natural reservoir for many coronaviruses. Intriguingly, we observed a lower cytosine content for the four human established epidemic viruses (HCoV-HKU1, 13.0%; HCoV-NL63, 14.4%; HCoV-OC43, 15.2%; HCoV-229E, 16.7%)

than the three spillover-related viruses infecting humans (SARS-CoV, 20.0%; MERS-CoV, 20.3%; SARS-CoV-2, 18.4%) and most bat viruses. The four human epidemic viruses have been established in human populations for decades. The significantly low cytosine content observed for these two viruses may indicate host-related features impacting cytosine-containing metabolites availability. Several studies of the codon usage biases in emerging coronaviruses have been published, providing a general view of the situation (see, e.g., Tort et al. 2020), without, however, exploring the contextual constraints in terms of metabolic properties of their hosts.

If the adaptation of coronaviruses to the human species was to drive down the cytosine level in the virus genome, then we might expect the cytosine content of SARS-CoV-2 strains to decrease as the epidemic unfolds. Our regression model is consistent with this view (fig. 3).

It allowed us to estimate that SARS-CoV-2 may lose its C complement by 0.000516 base per position per year ($y = -0.000516x + 1.226$, adjusted $R^2 = 0.1459$) while gaining U by 0.000634 per year ($y = 0.000634x - 0.9591$, adjusted $R^2 = 0.1835$), under its current circulation dynamics in susceptible populations. A parallel increased trend for A and a decrease for G was also observed, but with more moderate slopes than those for C and U. A Wilcoxon rank-sum test showed that the content of the four bases in the SARS-CoV-2 sequences was significantly different in each case, whereas somewhat correlated with each other. The strongest correlations were observed between two groups (supplementary fig. S2, Supplementary Material online): a decrease in A was significantly correlated with an increase in G (adjusted $R^2 = 0.5738$), whereas a decrease in C was significantly correlated with an increase in U (adjusted $R^2 = 0.7177$). As a consequence the SARS-CoV-2 virus is on its way to gradually lose C during its adaptation in humans, resulting in a genomic base composition more like those of the four previously established human endemic coronaviruses.

The second approach did not aim at creating a phylogeny of the viruses, but, rather, a cladistic tree showing structural properties shared by viruses likely to underlie functional features. This approach assumes that, after sufficient time of evolution, the nucleotides present at the majority of sites in the sequence had chances to be modified several times reaching local saturation, so that it is difficult or impossible to link those with specific features of the proteins encoded in the virus (the beginning and end of the sequence, critical for RNA-dependent replication are not taken into account). By contrast, the presence of insertions or deletions (indels) will affect considerably the overall structure of the proteins, and this should impact their function in a way that is not likely to be reversible (Zhou et al. 2020). An earlier such report (Sekowska et al. 2000) demonstrated the usefulness of this approach (Gupta 1998). The use of cladograms in this case attempts
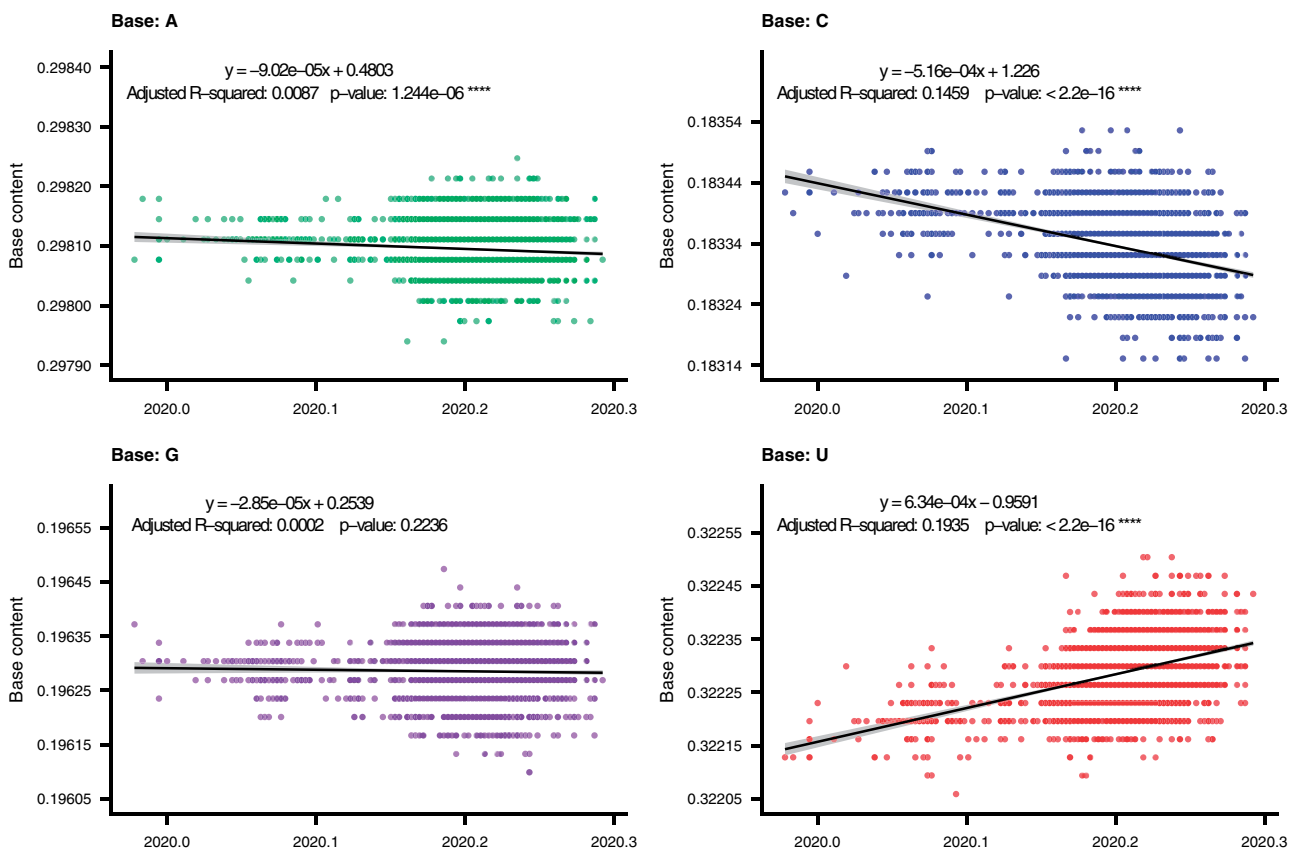
Fig. 3.—Dynamic of base composition at the coding regions of SARS-CoV-2. The base composition of the coding regions concatenated by 26 ORFs of SARS-CoV-2 is displayed. Each dot represents one sequence. The calculation was based on 2,574 unique SARS-CoV-2 strains isolated from December 24, 2010 to April 17, 2020.

to show the relative distances and should not necessarily reflect the evolutionary history of the group.

Compared with the standard alignment of the 89 reference genomes (supplementary table S1 and fig. S1, Supplementary Material online), the equivalent gap-based alignment uses undefined characters for nucleotides and "dummy" characters for gaps to cheat the algorithms for tree construction so that distances are calculated on the basis of the sums of scores for gap positions (presence of indels, see Materials and Methods). Although it is not possible to check one by one each and every gap, the common ones are likely to reflect a common structure or function characteristic of the corresponding region (fig. 4).

Remarkably, both the standard, genome-based tree and the gap-based tree are quite congruent—i.e., knowing only the indel content is enough to draw a tree that describes the relationships between the coronavirus groups (fig. 4). In the genome-based tree, the four groups of coronaviruses are detected clearly, and the seven human virus strains are highlighted, in groups alpha and beta (fig. 4A). In the gap/indel-based tree, the four groups are also consistently derived, with the exception of a beta subgroup that contains the two human viruses with reduced pathogenicity potential,

compared with the beta subgroup that contains the SARS, MERS, and SARS-2 strains (fig. 4B). At the same time, a tiny alpha subgroup exhibits similar indel patterns with the latter beta subgroup, presumably with similar indel patterns. It is tempting to speculate that these alpha subgroup strains may share certain hitherto unknown properties that might render them potentially dangerous in terms of zoonotic disease capacity. The observed patterns could be interpreted as showing that what is coded in the indel regions has a considerable weight on the virus adaptation to their hosts and does not strictly depend on the base composition and amino acid-coding potential of the genome sequences. More research is needed to establish the nature of indel-based trees in the future.

Biased Codon Composition of the Regions Coding for Individual Viral Proteins

Coronaviruses, and many positive-sense single-stranded RNA viruses as well, produce plus strands at a 50- to 100-fold excess of their minus-strand replicated template. Because several regions in the 3′ half of the virus are "transcribed" from the template RNA minus strand of the virus (Yang and
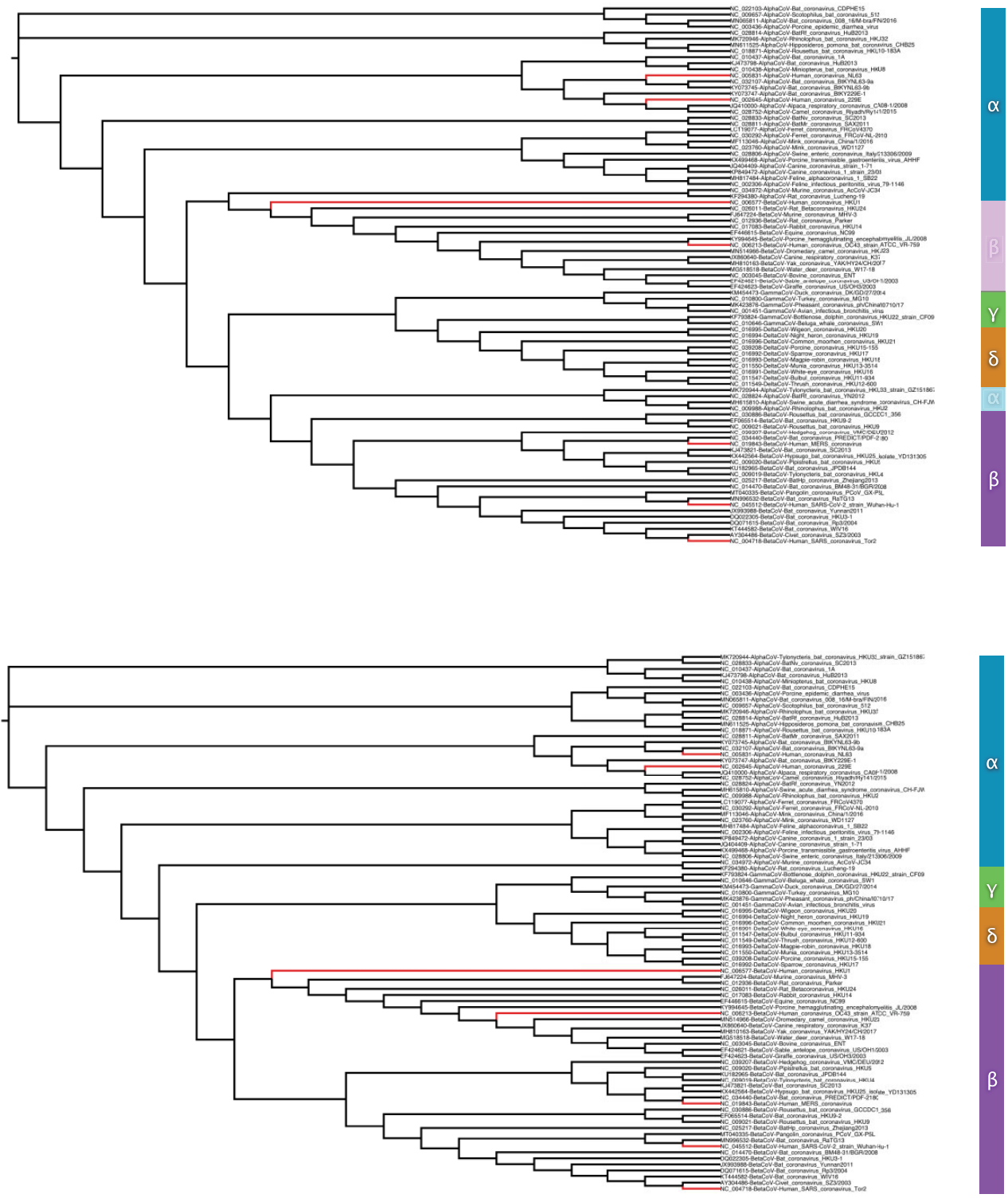
Fig. 4.—Phylogeny of coronavirus representatives based on full-genome sequences (upper panel) and on indels (lower panel). A genome-based tree is generated based on the full-genome sequence alignment of the group (upper panel) and a gap-based tree is created, based on insertions and deletions (indels) only (see Materials and Methods). The seven known human coronavirus strains are highlighted by a red color for the corresponding branches. A panel on the right indicates the four coronavirus groups; in lower panel, the two incongruent subgroups are shown by the same color code with reduced opacity (alpha and beta subgroups). For details, please see text.

Leibowitz 2015), a further deviation from parity should appear in the nucleotide usage for virus construction. This means that the overall nucleotide consumption is not strictly constrained by the second Chargaff's parity rule, that would result in an amount of A equal to that of U, and G to that of C (Forsdyke and Mortimer 2000). The virus multiplication rests on a RNA-dependent replication process, so that any pressure on a given base availability—here C—would affect its complement—G in our case. As discussed in the previous section, we expected a general selection pressure operating on CTP and tending, in the long run, to decrease the C content of the RNA virus, but also that of G.

Furthermore, this implies a particular imbalance in the nucleotide composition of the viral RNA, allowing it to differ from standard mRNAs of the host cell. We therefore expect that the virus will interfere with the host's translation machinery in a way that allows it to be discriminated positively against the cell's mRNAs (see Discussion). This should have consequences for the translation of the viral genome. The virus encodes proteins that have essential functions for its development, not only for the replication machinery and the formation of a capsid but also for several ancillary functions needed for hijacking the host metabolism. The constraint on the genome nucleotide composition must be reflected in the codon usage bias of the virus protein-coding sequences, with important consequences on the way tRNAs are used. Furthermore, because natural selection acts on viral functions, it can be expected that the outcome of the general C lowering trend will differ in different proteins encoded by the virus, depending on the selection pressure constraining their functions. Taking advantage of the degeneracy of the genetic code, SARS-CoV-2 could also limit its C content via the use of alternatives at the third codon position by selective codon usage.

To explore this hypothesis, the relative synonymous codon usage (RSCU) values were calculated for each coding region of SARS-CoV-2 to reveal any differential usage of synonymous codons. An RSCU value of 0, 0~0.6, 0.6–1.6, or >1.6 implies that a codon is not-used, underrepresented, normally used, or overrepresented—respectively, for the four value ranges (Uddin and Chakraborty 2017). Among the 26 major coding regions, six (Nsp11, ORF10, ORF7b, ORF6, E, and Nsp7) have a translated peptide length of <100 amino acids, which would result in codon usage profiles of low statistical significance. For example, Nsp11 encodes only 33 amino acids, which explains the very limited number of codons utilized by the corresponding gene. These sequences were not further analyzed (fig. 5). The three codon positions do not have the same importance in the selection of specific amino acids. Pressure against C must have consequences in terms of the protein-coding landscape of the virus. In general, in regions where tRNA choice allows a wobble between U and C, the virus sequence is considerably enriched in U. It seems noteworthy that the codon usage bias and bias in tRNA choice differs between genes of the

human host and the virus genes, except for two viral proteins, accessory protein Nsp1 and nucleocapsid protein N, notwithstanding preference of U over C—e.g., preference for GGU and CGU codons in protein Nsp1 (supplementary fig. S3, Supplementary Material online).

The first C codon position is used to input histidine, glutamine, proline, and arginine or leucine in proteins. This is particularly significant for the proline residue, essential in the folding of key viral protein domains, because it is encoded by CCN codons. All proteins of SARS-CoV-2 prefer the usage of CCA or CCU codons for proline, avoiding the usage of C and G (fig. 5). Histidine and glutamine are in two-codon boxes, discussed below. Arginine presents a different situation because CGN codons can be replaced by AGR codons: SARS-CoV-2 favors the AGA codon especially, with only one compulsory G. AGG codons are enriched in proteins Nsp5, Nsp8, and Nsp9. Remarkably, however, the Nsp1 protein, which corresponds to the initial domain of the ORF1a(b) protein, and is translated very early on in the virus expression cycle, contains only CGH codons (H = A, U, or C) and this is in total contrast with the other viral proteins (except for Nsp10, yet this protein has only two arginine residues, making this observation possibly irrelevant). Codon CGG is only present 11 times in the coding sequences of the virus, suggesting that when present, it has been submitted to positive selection, possibly at a site important for the translation-coupled folding of the protein. The most interesting location of this codon is a doublet that corresponds to a four codon insertion in the spike protein of the virus. Finally, the pressure on leucine content is also lower. CUN codons are used to code for leucine, with the majority using codon CUU, but this amino acid can be introduced using the alternative UUR codons. Yet, UUA is used more frequently than UUG. UUG is relatively enriched in proteins Nsp6, Nsp8, ORF3a, and N (fig. 5 and supplementary fig. S3, Supplementary Material online).

In the second position requiring a C, we find proline again, and also threonine (ACN), alanine (GCN), and serine (UCN). For threonine, codon ACU is the most used codon, progressively being generally replaced by ACA as we progress along the genome sequence, ACC and ACG are rare. Alanine is mainly encoded by GCU codons, followed by GCA, with protein Nsp1, again, differing somewhat from the other viral proteins in that the frequency of GCA and GCU are the same. Serine (UCN) is able to escape much of the constraint imposed by C availability as it can use the alternative AGY codons. Codons UCU and UCA are more or less used in an equivalent way, except, again, in protein Nsp1, which mainly uses AGU and AGC codons. In general, AGC is seldom used, whereas AGU is the dominant serine codon.

Finally, the third position can be replaced by A, U, or G in the four-codon boxes, two of which, valine and glycine, are further discussed below. In general, the corresponding NNC codons are rarely used. Again, protein Nsp1 is an exception, with codon GGC used more frequently than GGU. Overall
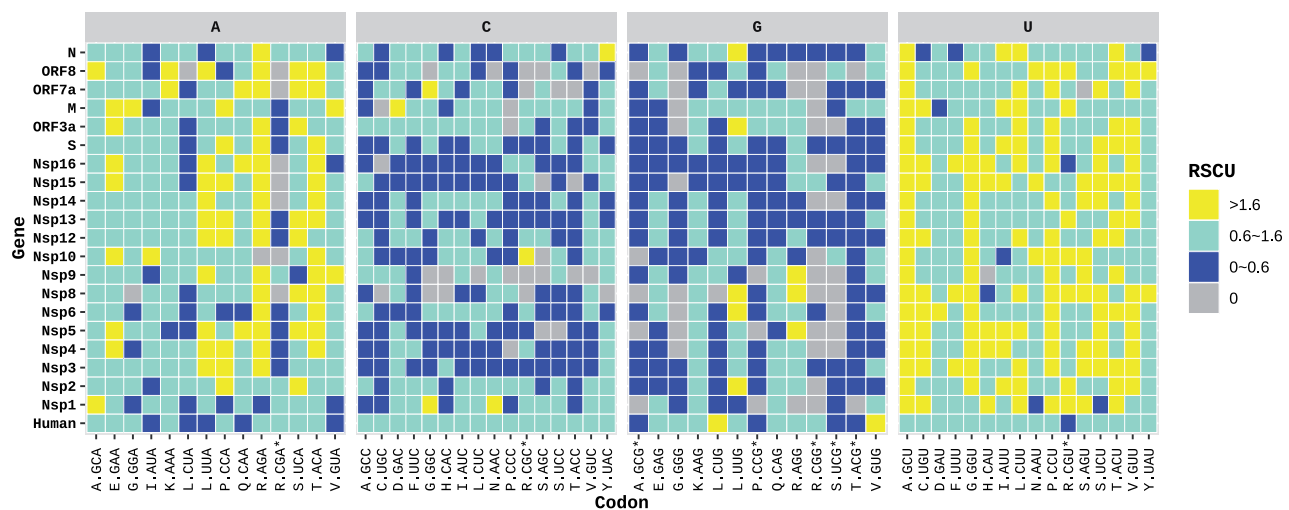
FIG. 5.—Codon usage of SARS-CoV-2 ORFs based on the third codon position compared with human-coding regions. The 20 SARS-CoV-2 ORFs with a length of over 300 nucleotides were submitted to RSCU calculation. The codon usage for 120,426 human-coding regions was also displayed to facilitate comparison. Codons are displayed with the first letter denoting the amino acid and the three letters following a dot representing the codon. Codons containing a CpG dinucleotide are suffixed by an asterisk. The four panels separate the codons according to the nucleotide located at the third codon position. Codons that are not used (RSCU = 0), underrepresented (RSCU < 0.6), normally utilized (RSCU ranges between 0.6 and 1.6), or overrepresented (RSCU > 1.6) are labeled in gray, blue, ice cold, and yellow, respectively.

GGU is dominating with some contribution of GGA, whereas GGG is often absent. In the case of valine (GUN codons), the dominating codon is GUU, followed by GUA. By contrast, U-ending codons which are rarer than expected are clustered in several proteins: UGU, UUU, and UAU in protein N; AUU in Nsp10; CGU in Nsp16; GAU in protein M, CAU in ORF8 and AAU and UCU in Nsp1. NAU codons correspond to two-codon boxes (NAN codons). These codons are discriminated along a pyrimidine/purine axis. A pyrimidine (NAY) is used to maintain the same nature of the coded residue whether the codon uses a U or a C as its 3'-end (aspartate, asparagine, histidine, and tyrosine), whereas a purine (NAR) allows coding for glutamate, glutamine, and lysine. UAR codons are also specifying the terminal step of translation. As stated above, the SARS-CoV-2 genes avoid the usage of C containing codons whenever possible (fig. 5). Moreover, probably due to the base-pairing requirement imposed during transcription and replication, the virus also avoids the usage of G-ending codons. This avoidance is maintained in the overall choice of NAR codons, except in protein Nsp6 where CAG is preferred to CAA, as well as GAG over GAA and CAA over CAG, which suggests that this results from a significant selection pressure. This is the more remarkable because Nsp proteins are cleaved off large ORF1a and ORF1ab precursors. In general, and this is as expected, codons NAU are preferred over NAC for the pyrimidine ending codons of NAN boxes. The exceptions are, for GAC, protein Nsp5 and protein M; for CAC, Nsp10 and ORF7a; for AAC, protein Nsp1 and protein M; and for UAC, proteins Nsp1, Nsp5, Nsp9, M, Orf7a, and N.

tRNA-Dependent Modulation of Synonymous Codon Translation

Consistent with metabolic pressure against CTP and despite their uneven coding length, most of the genes of SARS-CoV-2 avoid the usage of the C-ending codons (fig. 5 and supplementary fig. S3, Supplementary Material online). A similar low preference for C-ending codons was also observed for coronaviruses of other species and genera, as calculated using the ORF1ab coding region. The way tRNAs are utilized as a function of the first anticodon (third codon) nucleotide is highly unsymmetrical. For this reason, the corresponding tRNA position (N34) is usually heavily modified, whereas specific tRNAs are deciphering individual codons (table 2). Interestingly, this constraint is easily matched by the tRNA supply of the cell because, contrary to codons ending with a purine, which require distinct tRNAs to be decoded, codons ending with a pyrimidine (U or C, Y) are sometimes decoded by a common tRNA species. For NAY codons, the position 34 of tRNAs is a G, replaced by queuine (Q), if this metabolite of bacterial origin is present in the host. Availability of Q in the environment may not have major consequences for translation of NAC codons, but it may alter the speed and accuracy of translation of the NAU codons. G-ending codons are generally rare in the virus, but they do not systematically correspond to rare tRNAs (table 2). Because the anticodon position 34 of the cognate tRNAs is either a guanine or a queuine (Q) residue (depending on a specific input from the environment) and because NAU codons are translated in the absence of Q more slowly and less accurately than NAC codons, a pressure toward NAC in a

Table 2

Table of the Genetic Code with Emphasis on Decoding by Individual Human tRNAs

	A		G		U		C		
A	Gm (10)	Phe	I (9)	Ser	G/Q (13*)	Tyr	G [C32 mod Ψ, 29]	Cys	A
G									
U	×cm^5U (4)	Leu	ncm^5U (4)	Ser		ter		ter	
C	C (1 + 5*)	Leu	C (4)	Ser		ter	Cm (7)	Trp	
A	I (9)	Leu	I (9)	Pro	G/Q (10)	His	I (7)	Arg	G
G									
U	U (3)	Leu	ncm^5U (7)	Pro	×cm^5s^2U (6)	Gln	mcm^5U (6)	Arg	
C	C (9)	Leu	C (4)	Pro	C (13)	Gln	C (4)	Arg	
A	A (14)	Ile	I (9)	Thr	G/Q (20)	Asn	G (6)	Ser	U
G	G (3)	Ile							
U	Ψ (5*)	Ile	ncm^5U (6)	Thr	×cm^5s^2U (12)	Lys	×cm^5U (1 + 5*)	Arg	
C	C (9 + 1)	Met	C (5)	Thr	C(15)	Lys	C (5)	Arg	
A	I (9)	Val	I (22)	Ala	G/Q (13)	Asp	G (14)	Gly	C
G									
U	ncm^5U (5)	Val	ncm^5U (8)	Ala	×cm^5s^2U (7)	Glu	×cm^5Um (9)	Gly	
C	C (11)	Val	C (4)	Ala	C (8)	Glu	C (5)	Gly	

NOTE.—The table displays the distribution of the 415 tRNAs coded in the human genome, among which 28 (noted with an asterisk) must splice out an intron as a maturation step: 5 tRNA_Arg (decoding AGA), 5 tRNA_Leu (decoding UUG), 5 tRNA_Ile (decoding AUA), and 13 tRNA_Tyr (decoding UAC/UAU). Indication of modifications is provisional as many modifications are not yet biochemically identified in human cells (de Crécy-Lagard et al. 2019).

context where C availability seems to be limiting is probably significant. This may apply to protein Nsp1 and to a lesser extent to protein M (see Discussion). All tRNA decoding strategies depend on the type and extent of modifications at position 34 of the tRNA anticodon (Grosjean and Westhof 2016). The codon usage bias in SARS-CoV-2 differs from that of average human proteins. In particular, it is enriched in codons that require tRNAs modified at position N34 of the anticodon with complex modifications that are linked to zinc homeostasis (Danchin et al. 2020), an important feature knowing that several of the virus functions are Zn^{2+}-dependent, whereas antiviral protein ZAP is a zinc-finger protein (Meagher et al. 2019).

A prominent feature is that two A-ending codons, CUA and CGA are generally rare in the virus sequence (fig. 5 and supplementary fig. S3, Supplementary Material online). This is significant, as witnessed by the facts that the cognate codons CUU and CGU are particularly frequent (remember that A and U are both abundant in the virus genome). CUA is decoded by a specific tRNA_Leu which is subject to specific regulation (Frias et al. 2013). An exception is, as reported above, the AGA codon, which is particularly frequent, and this makes protein Nsp1 stand out, highlighting further A-ending codon deficiencies (GGA, CUA, CCA, AGA, and GUA). The deficiency of A-ending codons for nucleocapsid protein N, which is very rich in arginine residues and has the expected excess of AGA is limited to UUA, AUA, CUA, and GUA, which corresponds to a UpA deficiency in mammalian genomes (Belalov and Lukashev 2013).

Although the virus must certainly manage tRNA availability and adapt this resource to its specific codon usage bias, it must also curb the innate antiviral immunity which affects the pool of tRNAs directly. In human cells, tRNA molecules are synthesized as precursors that are matured into pre-tRNAs that lack their CCA-terminal end and need to be further modified (Slade et al. 2020). Remarkably, stress-induced synthesis of the specific protease angiogenin removes these CCA termini, stopping translation (Czech et al. 2013). Cells can overcome this process using tRNA nucleotidyltransferase and CTP and ATP. This is yet another CTP-controlled function that must be overcome by the virus. The specificity of angiogenin is modulated by tRNA modifications—this nuclease can also cut the tRNA molecules at sites located in their anticodons (Su et al. 2019)—and this may create an uneven selection pressure on the various tRNAs used to decode the virus genes.

Discussion

All viruses must tap into their host resources to build up multiple copies of their genome and their envelope. In the present study, we have documented the key role of CTP as a general coordinator of the cell's metabolism. This has unique consequences for the replication and evolution of enveloped RNA viruses, coronaviruses in particular. Metabolic availability of this nucleotide drives synthesis of the viral genome, its envelope, maintains the translation machinery, and controls protein glycosylation. This coordinated role makes us understand the presence of the general innate immunity antiviral metabolite, 3′-deoxy-3′,4′-didehydro-CTP (ddhCTP), produced from CTP by the interferon-induced protein viperin (Gizzi et al. 2018; Ebrahimi, Howie, et al. 2020). A general role of this unexpected metabolite has even been established in a work

published during revision of this article as important in the fight of prokaryotes against their phages (Bernheim et al. 2020). Indeed the role of ddhCTP has long been elusive, with experiments suggesting interference with RNA replication/transcription (Ng and Hiscox 2018), whereas others demonstrated interference with lipid metabolism (Nelp et al. 2017). It has also been shown that ddhCTP affects general metabolism via inhibition of NAD$^+$-dependent enzyme including the housekeeping enzyme glyceraldehyde-3-phosphate dehydrogenase (Ebrahimi, Vowles, et al. 2020). In this respect, it seems revealing th at *E. coli* CTP synthase is inhibited by NADH and other nicotinamides (Habrian et al. 2016). Cytoophidia have been observed to associate with IMP dehydrogenase to coordinate nucleotide metabolism (Chang et al. 2018; McCluskey and Bearne 2018) providing still another link between NAD-dependent enzymes and the multiplication of coronaviruses. No work, at this time, has shown that it should impact tRNA synthesis via inhibition of CCAse, a further action of this analog of CTP. How did this integrative role of CTP emerge during evolution?

Cells do not have to grow during viral infection. Yet, they result from billion years of evolution based on growth. The fate of the virus might therefore differ widely if the cells belong to classes that are normally poised to grow if triggered by relevant signals, or cells that are not meant to grow (such as neurons or cardiomyocytes). Accounting for growth in a 3D space—the physical space where material entities such as most cells flourish—this literally asks for squaring the circle because growth of the cytoplasm (three dimensions) must be matched with growth of the membrane (two dimensions) and growth of the genome (one dimension). Putting together these three facets while sharing a common metabolism cannot be straightforward. Alas, as often in biology, solving a clear functional problem results more often than not in ad hoc solutions built on a fairly haphazard collection of bits and pieces, with considerable differences between different species. This would then preclude any consistent view of the anecdotes invented during evolution and end up in a catalog of solutions, as witnessed in the millions of articles that tackle biological questions. We could anticipate that the extensive evolutionary time scale allowed for a slow progression, exploring an infinite variety of directions.

Yet, we could be—and have been—lucky, as we discovered a universal setup that may have some generality or even span the whole tree of life solving the growth hurdle. Because the number of the cell's building blocks is small (mainly nucleotides, amino acids, phospholipids, and carbohydrates), natural selection did recruit a limited number of those components to implement homeostatic regulation of the growth of the various cell compartments. From detailed analysis of the genome signatures of various organisms and their metabolic constraints, we have demonstrated here that the biosynthetic and salvage pathways leading to CTP had remarkable consequences in organizing core cellular functions. A first

pointer to this discovery was presented in Danchin and Marlière (2020) and a detailed view is now presented in figure 2. The highly involved setup of this metabolic facet is significant for the manner and process by which a virus invades a cell and subsequently evolves a progressively better-adapted progeny. Here, we explored, using a functional analysis approach, how understanding this exceptional setup of intermediary metabolism allowed us to anticipate this particular aspect of the evolution of RNA viruses. The main conclusion we reached is that, overall, the coronavirus genomes had a tendency to shed their cytosine—respectively guanine—complement, essentially replacing it by uracil—and to a lesser extent guanine by adenine.

Although this tendency constrains the genome as a whole, it is obvious that this will dramatically restrict the evolutionary trajectory of the virus, presumably leading to attenuation in the long term. Evolution, however, systematically uncovers negative counterparts for each novel function. This implies that the CTP-related armor defect constraining viral multiplication could be antagonized by specific viral functions, inactivating the interferon response or possibly specifically modulating the activity of CTP synthetase. This should be explored by metabolically focused studies of C-enrichment in some RNA viruses, such as that of the nonenveloped hepatitis E virus (Bouquet et al. 2012). In the case of SARS-CoV-2 and in the short term, because a major component of the antiviral innate immunity results from the production of the CTP analog ddhCTP, losing C residues in the genome will transiently alleviate some of the negative pressure created by this antiviral response. This also will help the virus to escape the limited, because it is highly context-dependent, deamination by APOBEC proteins (Milewska et al. 2018). A negative consequence of this genome composition trend might somehow account for the increase in virulence when a fairly GC-rich virus of an animal comes to infect a foreign host. Furthermore, occasional C-enrichment, resulting from inevitable template misreading, may be stabilized if the function of the corresponding translated polypeptide contributes to the production of a larger progeny of the virus. This makes identification of the functions associated to loci that do not readily comply with the loss of C (and G) residues as likely candidates important for a stable virus evolutionary potential.

Immediately upon internalization of the virus, its 3′-capped RNA genome begins to be translated into two large proteins coded from ORF1a and ORF1ab which contain a protease domain that cuts off 16 accessory proteins required for specific functions of the virus (Wang, Hu, et al. 2020). Its N-terminal domain, processed into nonstructural protein Nsp1, immediately interferes with translation of the host proteins—it is also inhibiting its own translation thus producing homeostatic regulation—by blocking the assembly of ribosomes that are in the process of translating host mRNAs

and disrupting nuclear-cytoplasmic transport (Gomez et al. 2019). Subsequently, a large complex forms with all the other Nsp proteins generated from the processed precursor, generating a RNA-dependent replication/transcription complex. Remarkably, this complex is tightly linked to key elements of the translation machinery. It has been demonstrated that, besides inhibition of interferon signaling, Nsp1 binds to the 40S ribosomal subunit (Kamitani et al. 2009) and that it further triggers host mRNA degradation (Narayanan et al. 2015). Nsp1 binds translation factors eIF3, eIF1A, eIF1, and eIF2-tRNAi-GTP (Thoms et al. 2020) and inhibits formation of the translation initiation complex—48S complex and formation of active 80S ribosomes (Lokugamage et al. 2012). Early interaction with the host translation machinery will stop translation, triggering host mRNA decay, which both produces nucleotide precursors for replication of the virus and hijacks the machinery to perform further translation of the viral genome. This implies that the complex between Nsp1 and the translation initiation complex is able to discriminate between different classes of mRNAs to allow or prevent their translation. Among the factors bound to Nsp1 the enigmatic ATP-dependent enzyme ABCE1 has been identified (Thoms et al. 2020). Remarkably, this protein is expected to behave as a "Maxwell's demon" as do proteins of the EttA family in Bacteria, allowing partition of specific mRNA families the expression of which needs to be coexpressed or corepressed (Boel et al. 2019).

This role of translation is apparent in the codon usage bias of Nsp1, which differs from that of subsequent domains cleaved off ORF1a and ORF1ab polypeptides. Here, the role of arginine residue codons seems to have been submitted to strong selection, with a majority being CGU codons, whereas AGA and AGG codons—AGA translation being overrepresented in the subsequent polypeptides—are totally absent from the sequence. In addition, the arginine codon CGG is extremely rare overall in the genome sequence, and its locations are revealing, likely to be important for the cotranslational folding of cognate proteins. This is particularly important in SARS-CoV-2 as the insertion generating its furin-like cleavage site in the spike protein that mediates cell entry (Follis et al. 2006; Belouzard et al. 2009; Coutard et al. 2020) is located right at a CGG doublet. Besides protein Nsp1, we demonstrated that the nucleocapsid protein N had also a general distribution of the codon usage bias that differed from that of the bulk of proteins coded from the ORF1a and ORF1ab regions. This is likely to be due to the fact that the corresponding transcripts also code for another protein in a different reading frame, protein ORF9b (Shi et al. 2014), and we can assume that this observation substantiates that this protein has indeed an important role in the biology of the virus. Remarkably, this also makes that the codon and tRNA

usage bias of protein N resembles that of the human host. Whether this is meaningful should be further explored.

Perspectives

Here, we reviewed the role of a specific intracellular metabolic pressure that must constrain the evolution of the genome sequence of RNA viruses, with emphasis on SARS-CoV-2 and in the context of the entire coronavirus family. Several studies have noticed the cytosine deficiency in the genome of evolving coronaviruses, with concomitant deficiency in the position of codons, but these observations were ascribed to deamination of cytosine resulting from the action of the host APOBEC system (Milewska et al. 2018) or to methylation of CpG dinucleotides (Wang, Mao, et al. 2020) as driving forces for evolution. By contrast, our working hypothesis is that the availability of CTP (and hence of cytosine-based precursors) is a dominating driving force in the way the virus evolves a new progeny. We are well aware that, due to the small number of samples and fairly short life time (as compared with usual evolutionary trajectory of a virus species), sequence analyses would provide only a limited view of sequence evolution and should be used more as a "rule of thumb" than a view based on trustworthy statistics. However, we believe that, in view of the urgent situation we are facing, it is important to communicate our observations while relating them to previously unrecognized pressure that must have considerable importance in the evolution of viruses and the metabolic backdrop of its biology in the host cell. In this respect, it seems worthwhile to explore whether unappreciated functions coded by viruses will be involved in controlling CTP availability.

Materials and Methods

Data Preparation

Data set of reference coronaviruses: viral genomes were downloaded from GenBank (https://www.ncbi.nlm.nih.gov/genbank/ last accessed November 9, 2020) and GISAID (https://www.gisaid.org/ last accessed November 9, 2020). Representative coronaviruses of different species were selected from complete genomes, with reference genomes recommended by the Coronaviridae Study Group of the International Committee on Taxonomy of Viruses (https://talk.ictvonline.org/ last accessed November 9, 2020) and NCBI retained preferentially. For viruses containing isolates from different hosts, at least one representative strain from each host was kept. The genomes were aligned using MAFFT v7.427 (Katoh et al. 2002) and manually checked with BioEdit. Alignment of full-genomic sequences was used for phylogeny reconstruction, whereas the coding regions for ORF1ab were extracted for codon usage analysis.

Data set of SARS-CoV-2: a total of 17,037 SARS-CoV-2-related sequences were available from GISAID on May 6, 2020 (Elbe and Buckland-Merrett 2017). Only SARS-CoV-2 genomes isolated from human, with a full length over 27,000 bp, no ambiguous sites, and detailed collection date information were used for alignment. For duplicate sequences, only the earliest isolate was kept. Sequences for 26 coding regions, including Nsp1, Nsp2, Nsp3, Nsp4, Nsp5, Nsp6, Nsp7, Nsp8, Nsp9, Nsp10, Nsp11, Nsp12, Nsp13, Nsp14, Nsp15, Nsp16, S, ORF3a, E, M, ORF6, ORF7a, ORF7b, ORF8, N, and ORF10 were extracted for each strain, using NC_045512 as reference. The coding sequences were checked manually to exclude those with abnormal mutations and early stop codons. A total of 4,110 strains with all 26 coding regions of complete ORF length were retained. After further deduplication based on the concatenated sequences comprised the 26 ORFs, the final data set contained a total of 2,574 unique SARS-CoV-2 isolates.

Phylogeny Reconstruction

Phylogenetic tree of the 89 representative coronaviruses was inferred using the maximum likelihood method implemented in IQ-TREE v1.6.12 with the GTR + F + I + G4 substitution model determined by ModelFinder (Nguyen et al. 2015; Kalyaanamoorthy et al. 2017; Hoang et al. 2018). Ultrafast bootstrap support values were calculated from 1,000 pseudoreplicate trees (Kalyaanamoorthy et al. 2017). Visualization of phylogenies was conducted with ggtree package (Yu 2020).

Gap-Based Alignment

The full alignment of the 89 reference strains was used to generate a tree, using FastTree 2.1.10 (Price et al. 2010) (with gamma distribution and the nucleotide option on—namely with the command options -gamma -nt), on the NGPhylogeny.fr server (Lemoine et al. 2019). The Jukes–Cantor model with balanced support Shimodaira–Hasegawa test was selected (Shimodaira and Hasegawa 1999). Total branch length was: 14.267.

Furthermore, a gap-based alignment was created, using gaps as follows: all dinucleotides were replaced with the "undefined" symbol "x" and the "dummy" symbols (W for 3, Y for 6, and F for 9 consecutive gaps and the V symbol for all single gaps), leaving only single-nucleotides in-between gaps as anchor points (7% of total). The encoding in gaps of 3/6/9 is used to emulate the importance of potential codon gaps (reflected in the BLOSUM45 matrix). Total branch length was: 1.673.

Gap-based genome-based phylogenetic reconstruction for this group is based on the fact that, as also mentioned recently elsewhere (Li et al. 2020), these viruses undergo significant recombination and a large number of nucleotide positions achieve saturation thus confounding phylogenetic signal. Tree visualization was facilitated by IcyTree (Vaughan 2017).

Base Content Calculation

Base content was calculated by dividing the occurrence of each base by the total length of the sequence. Genomic base contents of representative coronaviruses were calculated with the full viral genome sequences. For the base content dynamic analysis of SARS-CoV-2, base compositions were calculated using the 2,754 unique sequences concatenated by 26 ORFs.

Codon Usage Analysis

Codon usage analysis was conducted based on the ORF1ab region of representative coronaviruses and the 26 individual ORFs of SARS-CoV-2 strains. RSCU value was defined as the ratio of the observed codon usage to the expected value (Sharp and Li 1986). Codons with an RSCU value of 0, 0–0.6, 0.6–1.6, or >1.6 were regarded as not-used, underrepresented, normally used, or overrepresented (Uddin 2017). RSCUs for the 120,426 human-coding regions were determined based on the *Homo sapiens* codon usage table retrieved on June 14, 2020 from TissueCoCoPUTs (Kames et al. 2020).

Statistical Analysis and Plots

Statistical test, linear regression, and data visualization were all conducted in R. Kruskal–Wallis test by rank and Wilcoxon rank-sum test for pairwise comparisons were applied as appropriate. P values are labeled as follows: <0.0001, ****; 0.0001–0.001, ***; 0.001–0.01, **; 0.01–0.05, *; ≥0.05, not labeled. $P < 0.05$ was considered as significant.

Supplementary Material

Supplementary data are available at *Genome Biology and Evolution* online.

analysis of the cytosine complement of the virus and to Agnieszka Sekowska for her comments on metabolic pathways. We thank all the authors who shared genomic data in public database, and an acknowledgment table for sequences retrieved from GISAID (Elbe and Buckland-Merrett 2017) is provided (supplementary table S2, Supplementary Material online).

Author Contributions

A.D. designed the study and wrote the bulk of the article. Z.O., J.L., and W.C. developed the in silico analyses of cytosine evolution, codon usage biases, and phylogeny. Z.O., D.W., and W.S. performed the analysis and Z.O. wrote the corresponding part of the article. C.O. designed and performed phylogenetic studies based on indels. P.M. identified several steps of CTP metabolism critical for virus proliferation. All authors read, wrote some sections, and contributed to the final version of the article.

Conflict of Interest

A.D. is a founder of Stellate Therapeutics, a company developing applications of metabolism for prevention and cure of neurodegenerative diseases and a founder of Virtexx, a company developing antiviral molecules. Z.O. and authors from Shenzhen are employed by the BGI, a company developing applications of genome studies. P.M. is a founder of Theraxen, a company developing synthetic biology approaches for drug development. The other authors declare no conflict of interest.

Data Availability

A first version of this article has been deposited at bioRxiv repository under the reference https://biorxiv.org/cgi/content/short/2020.06.20.162933v1.

Literature Cited

Aldritt SM, Tien P, Wang CC. 1985. Pyrimidine salvage in *Giardia lamblia*. J Exp Med. 161(3):437–445.

Arribas M, Aguirre J, Manrubia S, Lázaro E. 2018. Differences in adaptive dynamics determine the success of virus variants that propagate together. Virus Evol. 4(1):vex043.

Arrivault S. 2019. UMP pyrophosphorylase: a moonlighting protein with essential functions in chloroplast development and photosynthesis establishment. Plant Physiol. 180(4):1779–1780.

Ashihara H, Stasolla C, Fujimura T, Crozier A. 2018. Purine salvage in plants. Phytochemistry 147:89–124.

Aurrecoechea C, et al. 2009. GiardiaDB and TrichDB: integrated genomic resources for the eukaryotic protist pathogens *Giardia lamblia* and *Trichomonas vaginalis*. Nucleic Acids Res. 37(Database):D526–D530.

Balendiran GK, et al. 1999. Ternary complex structure of human HGPRTase, pRpp, Mg^{2+}, and the inhibitor HPP reveals the involvement of the flexible loop in substrate binding. Protein Sci. 8(5):1023–1031.

Belalov IS, Lukashev AN. 2013. Causes and implications of codon usage bias in RNA viruses. PLoS One 8(2):e56642.

Belouzard S, Chu VC, Whittaker GR. 2009. Activation of the SARS coronavirus spike protein via sequential proteolytic cleavage at two distinct sites. Proc Natl Acad Sci U S A. 106(14):5871–5876.

Bernheim A, et al. 2020. Prokaryotic viperins produce diverse antiviral molecules. Nature doi: 10.1038/s41586-020-2762-2.

Boel G, Danot O, de Lorenzo V, Danchin A. 2019. Omnipresent Maxwell's demons orchestrate information management in living cells. Microb Biotechnol. 12(2):210–242.

Bouquet J, Cherel P, Pavio N. 2012. Genetic characterization and codon usage bias of full-length Hepatitis E virus sequences shed new lights on genotypic distribution, host restriction and genome evolution. Infect Genet Evol. 12(8):1842–1853.

Chang C-C, Keppeke GD, Sung L-Y, Liu J-L. 2018. Interfilament interaction between IMPDH and CTPS cytoophidia. FEBS J. 285(20):3753–3768.

Chauhan N, Farine L, Pandey K, Menon AK, Bütikofer P. 2016. Lipid topogenesis – 35years on. Biochim Biophys Acta. 1861(8):757–766.

Chen Y, Liu Q, Guo D. 2020. Emerging coronaviruses: genome structure, replication, and pathogenesis. J Med Virol. 92(4):418–423.

Cheng M-L, et al. 2020. Metabolic reprogramming of host cells in response to enteroviral infection. Cells 9(2):473.

Cleary MD, Meiering CD, Jan E, Guymon R, Boothroyd JC. 2005. Biosynthetic labeling of RNA with uracil phosphoribosyltransferase allows cell-specific microarray analysis of mRNA synthesis and decay. Nat Biotechnol. 23(2):232–237.

Corman VM, et al. 2015. Evidence for an ancestral association of human coronavirus 229E with bats. J Virol. 89(23):11858–11870.

Coutard B, et al. 2020. The spike glycoprotein of the new coronavirus 2019-nCoV contains a furin-like cleavage site absent in CoV of the same clade. Antiviral Res. 176:104742.

Cui J, Li F, Shi Z-L. 2019. Origin and evolution of pathogenic coronaviruses. Nat Rev Microbiol. 17(3):181–192.

Czech A, Wende S, Mörl M, Pan T, Ignatova Z. 2013. Reversible and rapid transfer-RNA deactivation as a mechanism of translational repression in stress. PLoS Genet. 9(8):e1003767.

Dai YP, Lee CS, O'Sullivan WJ. 1995. Properties of uracil phosphoribosyltransferase from *Giardia intestinalis*. Int J Parasitol. 25(2):207–214.

Danchin A. 2009. Natural selection and immortality. Biogerontology 10(4):503–516.

Danchin A, Marlière P. 2020. Cytosine drives evolution of SARS-CoV-2. Environ Microbiol. 22(6):1977–1985.

Danchin A, Sekowska A, You C. 2020. One-carbon metabolism, folate, zinc and translation. Microb Biotechnol. 13(4):899–925.

de Crécy-Lagard V, et al. 2019. Matching tRNA modifications in humans to their known and predicted enzymes. Nucleic Acids Res. 47(5):2143–2159.

Del Caño-Ochoa F, Ramón-Maiques S. 2020. The multienzymatic protein CAD leading the de novo biosynthesis of pyrimidines localizes exclusively in the cytoplasm and does not translocate to the nucleus. Nucleosides Nucleotides Nucleic Acids 30:1–15.

Di Giorgio S, Martignano F, Torcia MG, Mattiuz G, Conticello SG. 2020. Evidence for host-dependent RNA editing in the transcriptome of SARS-CoV-2. Sci Adv. 6(25):eabb5813.

Donini S, Ferraris DM, Miggiano R, Massarotti A, Rizzi M. 2017. Structural investigations on orotate phosphoribosyltransferase from *Mycobacterium tuberculosis*, a key enzyme of the de novo pyrimidine biosynthesis. Sci Rep. 7(1):1180.

Drosten C, Preiser W, Günther S, Schmitz H, Doerr HW. 2003. Severe acute respiratory syndrome: identification of the etiological agent. Trends Mol Med. 9(8):325–327.

Ducati RG, Breda A, Basso LA, Santos DS. 2011. Purine salvage pathway in *Mycobacterium tuberculosis*. Curr Med Chem. 18(9):1258–1275.

Ebrahimi KH, Howie D, et al. 2020. Viperin, through its radical-SAM activity, depletes cellular nucleotide pools and interferes with

mitochondrial metabolism to inhibit viral replication. FEBS Lett. 594(10):1624–1630.

Ebrahimi KH, Vowles J, Browne C, McCullagh J, James WS. 2020. ddhCTP produced by the radical-SAM activity of RSAD2 (viperin) inhibits the NAD+-dependent activity of enzymes to modulate metabolism. FEBS Lett. 594(10):1631–1644.

Elbe S, Buckland-Merrett G. 2017. Data, disease and diplomacy: GISAID's innovative contribution to global health: data, disease and diplomacy. Glob Chall. 1(1):33–46.

Follis KE, York J, Nunberg JH. 2006. Furin cleavage of the SARS coronavirus spike glycoprotein enhances cell-cell fusion but does not affect virion entry. Virology 350(2):358–369.

Forsdyke DR, Mortimer JR. 2000. Chargaff's legacy. Gene 261(1):127–137.

Frances A, Cordelier P. 2020. The emerging role of cytidine deaminase in human diseases: a new opportunity for therapy? Mol Ther. 28(2):357–366.

Frias D, et al. 2013. Human retrovirus codon usage from tRNA point of view: therapeutic insights. Bioinform Biol Insights. 7:BBI.S12093–345.

Furusho K, et al. 2019. Cytidine deaminase enables Toll-like receptor 8 activation by cytidine or its analogs. Int Immunol. 31(3):167–173.

Ghérardi A, Sarciron M-E. 2007. Molecules targeting the purine salvage pathway in Apicomplexan parasites. Trends Parasitol. 23(8):384–389.

Ghosh AC, Shimell M, Leof ER, Haley MJ, O'Connor MB. 2015. UPRT, a suicide-gene therapy candidate in higher eukaryotes, is required for Drosophila larval growth and normal adult lifespan. Sci Rep. 5(1):13176.

Gizzi AS, et al. 2018. A naturally occurring antiviral ribonucleotide encoded by the human genome. Nature 558(7711):610–614.

Gomez GN, Abrar F, Dodhia MP, Gonzalez FG, Nag A. 2019. SARS coronavirus protein nsp1 disrupts localization of Nup93 from the nuclear pore complex. Biochem Cell Biol. 97(6):758–766.

Grolla AA, et al. 2020. A nicotinamide phosphoribosyltransferase-GAPDH interaction sustains the stress-induced NMN/NAD+ salvage pathway in the nucleus. J Biol Chem. 295(11):3635–3651.

Grosjean H, Westhof E. 2016. An integrated, structure- and energy-based view of the genetic code. Nucleic Acids Res. 44(17):8020–8040.

Gupta RS. 1998. Protein phylogenies and signature sequences: a reappraisal of evolutionary relationships among archaebacteria, eubacteria, and eukaryotes. Microbiol Mol Biol Rev. 62(4):1435–1491.

Habrian C, et al. 2016. Inhibition of Escherichia coli CTP synthetase by NADH and other nicotinamides and their mutual interactions with CTP and GTP. Biochemistry 55(39):5554–5565.

Hew K, et al. 2015. Structure of the varicella zoster virus thymidylate synthase establishes functional and structural similarities as the human enzyme and potentiates itself as a target of brivudine. PLoS One 10(12):e0143947.

Hoang DT, Chernomor O, von Haeseler A, Minh BQ, Vinh LS. 2018. UFBoot2: improving the ultrafast bootstrap approximation. Mol Biol Evol. 35(2):518–522.

Hutchison CA, et al. 2016. Design and synthesis of a minimal bacterial genome. Science 351(6280):aad6253.

Huynh J, et al. 2012. Evidence supporting a zoonotic origin of human coronavirus strain NL63. J Virol. 86(23):12816–12825.

Ireton GC, McDermott G, Black ME, Stoddard BL. 2002. The structure of Escherichia coli cytosine deaminase. J Mol Biol. 315(4):687–697.

Jarroll EL, Manning P, Berrada A, Hare D, Lindmark DG. 1989. Biochemistry and metabolism of Giardia. J Protozool. 36(2):190–197.

Jenkins GM, Pagel M, Gould EA, Zanotto P. D A, Holmes EC. 2001. Evolution of base composition and codon usage bias in the genus Flavivirus. J Mol Evol. 52(4):383–390.

Jin X, et al. 2013. Characterization of the guanine-N7 methyltransferase activity of coronavirus nsp14 on nucleotide GTP. Virus Res. 176(1-2):45–52.

Kalyaanamoorthy S, Minh BQ, Wong TKF, von Haeseler A, Jermiin LS. 2017. ModelFinder: fast model selection for accurate phylogenetic estimates. Nat Methods. 14(6):587–589.

Kames J, et al. 2020. TissueCoCoPUTs: novel human tissue-specific codon and codon-pair usage tables based on differential tissue gene expression. J Mol Biol. 432(11):3369–3378.

Kamitani W, Huang C, Narayanan K, Lokugamage KG, Makino S. 2009. A two-pronged strategy to suppress host protein synthesis by SARS coronavirus Nsp1 protein. Nat Struct Mol Biol. 16(11):1134–1140.

Kanehisa M, Furumichi M, Tanabe M, Sato Y, Morishima K. 2017. KEGG: new perspectives on genomes, pathways, diseases and drugs. Nucleic Acids Res. 45(D1):D353–D361.

Katahira R, Ashihara H. 2002. Profiles of pyrimidine biosynthesis, salvage and degradation in disks of potato (Solanum tuberosum L.) tubers. Planta 215(5):821–828.

Katoh K, Misawa K, Kuma K, Miyata T. 2002. MAFFT: a novel method for rapid multiple sequence alignment based on fast Fourier transform. Nucleic Acids Res. 30(14):3059–3066.

Khrustalev VV, Barkovsky EV. 2011. Unusual nucleotide content of Rubella virus genome as a consequence of biased RNA-editing: comparison with Alphaviruses. Int J Bioinform Res Appl. 7(1):82–100.

Kuo L, Koetzner CA, Masters PS. 2016. A key role for the carboxy-terminal tail of the murine coronavirus nucleocapsid protein in coordination of genome packaging. Virology 494:100–107.

Kutnjak D, Elena SF, Ravnikar M. 2017. Time-sampled population sequencing reveals the interplay of selection and genetic drift in experimental evolution of potato virus Y. J Virol. 91:e00690-17.

Lau SKP, et al. 2015. Discovery of a novel coronavirus, China rattus coronavirus HKU24, from Norway rats supports the murine origin of betacoronavirus 1 and has implications for the ancestor of betacoronavirus lineage A. J Virol. 89(6):3076–3092.

Lee J, Ridgway ND. 2020. Substrate channeling in the glycerol-3-phosphate pathway regulates the synthesis, storage and secretion of glycerolipids. Biochim Biophys Acta Mol Cell Biol Lipids. 1865(1):158438.

Lemoine F, et al. 2019. NGPhylogeny.fr: new generation phylogenetic services for non-specialists. Nucleic Acids Res. 47(W1):W260–W265.

Li F. 2016. Structure, function, and evolution of coronavirus spike proteins. Annu Rev Virol. 3(1):237–261.

Li H, et al. 2018. Active transport of cytoophidia in Schizosaccharomyces pombe. FASEB J. 32(11):5891–5898.

Li J, et al. 2007. Identification and characterization of human uracil phosphoribosyltransferase (UPRTase). J Hum Genet. 52(5):415–422.

Li X, et al. 2020. Emergence of SARS-CoV-2 through recombination and strong purifying selection. Sci Adv. 6(27):eabb9153.

Liu J-L. 2010. Intracellular compartmentation of CTP synthase in Drosophila. J Genet Genomics. 37(5):281–296.

Lokugamage KG, Narayanan K, Huang C, Makino S. 2012. Severe acute respiratory syndrome coronavirus protein nsp1 is a novel eukaryotic translation inhibitor that represses multiple steps of translation initiation. J Virol. 86(24):13598–13608.

Lucas-Hourani M, et al. 2013. Inhibition of pyrimidine biosynthesis pathway suppresses viral growth through innate immunity. PLoS Pathog. 9(10):e1003678.

Lüscher A, Lamprea-Burgunder E, Graf FE, de Koning HP, Mäser P. 2014. Trypanosoma brucei adenine-phosphoribosyltransferases mediate adenine salvage and aminopurinol susceptibility but not adenine toxicity. Int J Parasitol Drugs Drug Resist. 4(1):55–63.

Maldonado EN, Lemasters JJ. 2014. ATP/ADP ratio, the missed connection between mitochondria and the Warburg effect. Mitochondrion 19:78–84.

Martin E, et al. 2020. Impaired lymphocyte function and differentiation in CTPS1-deficient patients result from a hypomorphic homozygous mutation. JCI Insight 5(5):e133880.

Mayer KA, Stöckl J, Zlabinger GJ, Gualdoni GA. 2019. Hijacking the supplies: metabolism as a novel facet of virus-host interaction. Front Immunol. 10:1533.

McCluskey GD, Bearne SL. 2018. Anfractuous assemblies of IMP dehydrogenase and CTP synthase: new twists on regulation? FEBS J. 285(20):3724–3728.

McMaster CR. 2018. From yeast to humans – roles of the Kennedy pathway for phosphatidylcholine synthesis. FEBS Lett. 592(8):1256–1272.

Meagher JL, et al. 2019. Structure of the zinc-finger antiviral protein in complex with RNA reveals a mechanism for selective targeting of CG-rich viral sequences. Proc Natl Acad Sci U S A. 116(48):24303–24309.

Milewska A, et al. 2018. APOBEC3-mediated restriction of RNA virus replication. Sci Rep. 8(1):5960.

Mitchell A, Finch LR. 1979. Enzymes of pyrimidine metabolism in Mycoplasma mycoides subsp. mycoides. J Bacteriol. 137(3):1073–1080.

Moreno A, et al. 2017. Detection and full genome characterization of two beta CoV viruses related to Middle East respiratory syndrome from bats in Italy. Virol J. 14(1):239.

Moreno-Altamirano MMB, Kolstoe SE, Sánchez-García FJ. 2019. Virus control of cell metabolism for replication and evasion of host immune responses. Front Cell Infect Microbiol. 9:95.

Narayanan K, Ramirez SI, Lokugamage KG, Makino S. 2015. Coronavirus nonstructural protein 1: common and distinct functions in the regulation of host and viral gene expression. Virus Res. 202:89–100.

Nelp MT, Young AP, Stepanski BM, Bandarian V. 2017. Human viperin causes radical SAM-dependent elongation of Escherichia coli, hinting at Its physiological role. Biochemistry 56(30):3874–3876.

Ng LFP, Hiscox JA. 2018. Viperin poisons viral replication. Cell Host Microbe 24(2):181–183.

Nguyen L-T, Schmidt HA, von Haeseler A, Minh BQ. 2015. IQ-TREE: a fast and effective stochastic algorithm for estimating maximum-likelihood phylogenies. Mol Biol Evol. 32(1):268–274.

Orton RJ, Wright CF, King DP, Haydon DT. 2020. Estimating viral bottleneck sizes for FMDV transmission within and between hosts and implications for the rate of viral evolution. Interface Focus. 10(1):20190066.

Perrier A, et al. 2019. The C-terminal domain of the MERS coronavirus M protein contains a trans-Golgi network localization signal. J Biol Chem. 294(39):14406–14421.

Pratelli A, Colao V. 2015. Role of the lipid rafts in the life cycle of canine coronavirus. J Gen Virol. 96(2):331–337.

Price MN, Dehal PS, Arkin AP. 2010. FastTree 2 – approximately maximum-likelihood trees for large alignments. PLoS One 5(3):e9490.

Rasmussen UB, Mygind B, Nygaard P. 1986. Purification and some properties of uracil phosphoribosyltransferase from Escherichia coli K12. Biochim Biophys Acta. 881(2):268–275.

Rocha EP, Danchin A. 2002. Base composition bias might result from competition for metabolic resources. Trends Genet. 18(6):291–294.

Sawicki SG, Sawicki DL, Siddell SG. 2007. A contemporary view of coronavirus transcription. J Virol. 81(1):20–29.

Schoeman D, Fielding BC. 2019. Coronavirus envelope protein: current knowledge. Virol J. 16(1):69.

Schumacher MA. 1998. Crystal structures of Toxoplasma gondii uracil phosphoribosyltransferase reveal the atomic basis of pyrimidine discrimination and prodrug binding. EMBO J. 17(12):3219–3232.

Sekowska A, Ashida H, Danchin A. 2019. Revisiting the methionine salvage pathway and its paralogues. Microb Biotechnol. 12(1):77–97.

Sekowska A, Danchin A, Risler JL. 2000. Phylogeny of related functions: the case of polyamine biosynthetic enzymes. Microbiology 146 (8):1815–1828.

Sharp PM, Li W-H. 1986. An evolutionary perspective on synonymous codon usage in unicellular organisms. J Mol Evol. 24(1–2):28–38.

Shi C-S, et al. 2014. SARS-coronavirus open reading frame-9b suppresses innate immunity by targeting mitochondria and the MAVS/TRAF3/TRAF6 signalosome. J Immunol. 193(6):3080–3089.

Shimodaira H, Hasegawa M. 1999. Multiple comparisons of log-likelihoods with applications to phylogenetic inference. Mol Biol Evol. 16(8):1114–1116.

Shin Y, Hedglin M, Murakami KS. 2020. Structural basis of reiterative transcription from the pyrG and pyrBI promoters by bacterial RNA polymerase. Nucleic Acids Res. 48(4):2144–2155.

Shridas P, Waechter CJ. 2006. Human dolichol kinase, a polytopic endoplasmic reticulum membrane protein with a cytoplasmically oriented CTP-binding site. J Biol Chem. 281(42):31696–31704.

Slade A, Kattini R, Campbell C, Holcik M. 2020. Diseases associated with defects in tRNA CCA addition. Int J Mol Sci. 21(11):3780.

Song H-D, et al. 2005. Cross-host evolution of severe acute respiratory syndrome coronavirus in palm civet and human. Proc Natl Acad Sci U S A. 102(7):2430–2435.

Su Z, Kuscu C, Malik A, Shibata E, Dutta A. 2019. Angiogenin generates specific stress-induced tRNA halves and is not involved in tRF-3–mediated gene silencing. J Biol Chem. 294(45):16930–16941.

Sun Z, Liu J-L. 2019. mTOR-S6K1 pathway mediates cytoophidium assembly. J Genet Genomics. 46(2):65–74.

Thompson LR, et al. 2011. Phage auxiliary metabolic genes and the redirection of cyanobacterial host carbon metabolism. Proc Natl Acad Sci U S A. 108(39):E757–E764.

Thoms M, et al. 2020. Structural basis for translational shutdown and immune evasion by the Nsp1 protein of SARS-CoV-2. Science 369(6508):1249–1255.

Tort FL, Castells M, Cristina J. 2020. A comprehensive analysis of genome composition and codon usage patterns of emerging coronaviruses. Virus Res. 283:197976.

Uddin A. 2017. Indices of codon usage bias. J Proteomics Bioinform. 10(6):1000e34.

Uddin A, Chakraborty S. 2017. Synonymous codon usage pattern in mitochondrial CYB gene in pisces, aves, and mammals. Mitochondrial DNA A DNA Mapp Seq Anal. 28(2):187–196.

Vaughan TG. 2017. IcyTree: rapid browser-based visualization for phylogenetic trees and networks. Bioinformatics 33(15):2392–2394.

Villela AD, Sánchez-Quitian ZA, Ducati RG, Santos DS, Basso LA. 2011. Pyrimidine salvage pathway in Mycobacterium tuberculosis. Curr Med Chem. 18(9):1286–1298.

Wang L, Hu W, Fan C. 2020. Structural and biochemical characterization of SADS-CoV papain-like protease 2. Protein Sci. 29(5):1228–1241.

Wang Y, Mao J-M, et al. 2020. Human SARS-CoV-2 has evolved to reduce CG dinucleotide in its open reading frames. Sci Rep. 10(1):12331.

Wegelin I. 1983. Studies of pyrimidine metabolism during chick development: enzymes involved in CMP breakdown. Comp Biochem Physiol C Comp Pharmacol Toxicol. 75(2):391–393.

Wellen KE, Thompson CB. 2012. A two-way street: reciprocal regulation of metabolism and signalling. Nat Rev Mol Cell Biol. 13(4):270–276.

Westheimer FH. 1987. Why nature chose phosphates. Science 235(4793):1173–1178.

Wilson JM, et al. 1986. Human adenine phosphoribosyltransferase. Complete amino acid sequence of the erythrocyte enzyme. J Biol Chem. 261(29):13677–13683.

Woods PS, et al. 2016. Lethal H1N1 influenza A virus infection alters the murine alveolar type II cell surfactant lipidome. Am J Physiol Lung Cell Mol Physiol. 311(6):L1160–L1169.

Xia X. 2020. Extreme genomic CpG deficiency in SARS-CoV-2 and evasion of host antiviral defense. Mol Biol Evol. 37(9):2699–2705.

Yang D, Leibowitz JL. 2015. The structure and functions of coronavirus genomic 3' and 5' ends. Virus Res. 206:120–133.

Yang X-L, et al. 2016. Isolation and characterization of a novel bat coronavirus closely related to the direct progenitor of severe acute respiratory syndrome coronavirus. J Virol. 90(6):3253–3256.

Yong J, et al. 2019. Mitochondria supply ATP to the ER through a mechanism antagonized by cytosolic Ca2+. eLife 8:e49682.

Yu G. 2020. Using ggtree to visualize data on tree-like structures. Curr Protoc Bioinformatics. 69(1):e96.

Zauri M, et al. 2015. CDA directs metabolism of epigenetic nucleosides revealing a therapeutic window in cancer. Nature 524(7563):114–118.

Zhou H, et al. 2020. A novel bat coronavirus closely related to SARS-CoV-2 contains natural insertions at the S1/S2 cleavage site of the pike proteins. Curr Biol. 30(11):2196–2203.

Zhu Z, et al. 2016. Analysis of complete genomes of the rubella virus genotypes 1E and 2B which circulated in China, 2000–2013. Sci Rep. 6(1):39025.

Associate editor: Esther Angert